IEEE Access
Multidisciplinary | Rapid Review | Open Access Journal

Received March 3, 2021, accepted March 15, 2021, date of publication March 22, 2021, date of current version March 30, 2021.

*Digital Object Identifier 10.1109/ACCESS.2021.3068070*

# Constraint Waveform Design for Spectrum Sharing Under Coexistence of Radar and Communication Systems

**SULEMAN MIR[1], INAM BARI[2], (Senior Member, IEEE), MOHSIN KAMAL[1], (Senior Member, IEEE), AND HAIDER ALI[3], (Senior Member, IEEE)**

[1]Department of Electrical Engineering, National University of Computer and Emerging Sciences, Peshawar 25000, Pakistan
[2]Systems Engineering Department, Military Technological College, Muscat 111, Oman
[3]Department of Electrical and Electronics Engineering, University of Technology at Nowshera, Nowshera 24100, Pakistan

Corresponding author: Suleman Mir (suleman.mir@nu.edu.pk)

**ABSTRACT** Waveform design and spectrum sharing between Multiple Input Multiple Output (MIMO) radar and MIMO communication system is an optimization problem that has been typically addressed in literature with two-dimensional formalism involving radius and azimuth angles. In this paper, we address the problem and associated spectrum sharing constraints by the inclusion of an additional elevation angle. The design uses Finite Alphabet Constant Envelope (FACE) Binary Phase Shift Keying (BPSK) waveforms to formulate the covariance matrices. Through machine learning, a nonlinear optimization problem with constraints is converted to an optimization problem without constraints. The design criteria for the radar waveform does not interfere with the communication system. This is done by carefully selecting the base station (BS) and steering nulls towards it, which guarantees the least degradation in the radar's performance. We designed BPSK waveforms for spectral coexistence between MIMO radar and MIMO cellular communication system through different relaying protocols. Probability of detection and signal to noise ratio is formulated for different relaying protocols. The radar is capable of detecting a target in the air through azimuth as well as by elevation angle. We also showed that the desired covariance matrix is positive semi definite and radar can share the spectrum while detecting the target. We also showed a minimum square error for both angles based on the algorithm.

**INDEX TERMS**
Minimum square error, spectrum sharing techniques, cognitive radio cellular system, probability of detection.

## I. INTRODUCTION

Typically, the limited spectrum is allocated for commercial applications in contrast to the government or federal agencies [1]. According to the National Telecommunications and Information Administration (NTIA), commercial operators are assigned 7% of overall bandwidth [2]. The radio frequency spectrum is utilized for many aspects which include mobile communication, satellite communication, broadcasting, surveillance, federal aviation administration and many more. Commercial operators hence are facing bandwidth problem due to increasing number of users using smart phones and gadgets, creating the demand for high bandwidth [2]. With the increasing demand for broadband data over the last few years, there is a need for additional spectrum resources for cellular systems.

Mobile traffic will cross over from 7 Exabytes to 49 Exabytes by the end of 2021 [2]. This increase will be 47% of the compound annual growth rate. Bandwidth provided to federal agencies is underutilized compared to bandwidth provided to commercial systems. This inefficiency leads to the idea of sharing spectrum between different systems with minimal degradation to each other [3], [4]. As per [5], [6], different radars working at 3.4 GHz and 5.6 GHz can share the spectrum with LTE and WIFI systems in the near future. For spectrum sharing between radar and communication system, Electro Magnetic Interference (EMI) should be mitigated. Communication systems can cope with EMI but radar

The associate editor coordinating the review of this manuscript and approving it for publication was Mehmet Alper Uslu.

systems need more care due to sensitive receiver antennas. Four types of interference mitigation techniques are used for cancellation of the radar interference on the communication system, i.e., frequency, time, space, and system-level modification [7]. Practically, radar systems are more sensitive as they need to detect objects far away and hence, are more affected with interference from the communication system. For this purpose, a single antenna communication system should transmit a signal on the low power scale so that interference on a single radar system is minimal [8], [9], and [10].

Single radar technology has been changed to Multiple Input Multiple Output (MIMO) radars, and they are now more resilient to handle interference due to the knowledge of their Radio Environment Map (REM). Estimating the interference channel between MIMO radar and MIMO communication systems is carried out through search and track mode. The radar and communication systems are uncoordinated, and Base Station (BS) has to acquire Interference Channel State Information (ICSI) through radar probing waveforms. Both Line Of Sight (LOS) and Non-Line Of Sight (NLOS) channels are modelled through hypothesis testing techniques [11]. This advancement in radar systems created beam configuration approach to reduce the interference of MIMO radar communication system [12]. Different algorithms involving spatial domain is opted to avoid interference between different systems. The radar's signal is projected on the null space of MIMO communication system interfering single-channel, and zero interference is showed to occur in communication systems while pressuring radar performance [13].

Instead of a single interference channel, multiple channels can be considered between MIMO radar and communication systems. A new projection algorithm is used for the minimum degradation of performance between both systems [13], [14]. The optimization problem in [14] is termed as beam matching problem in which the designed beams are matched with the desired beams. The problem is solved by the synthesis of the covariance matrix of the waveform. Constant Envelop (CE) waveforms are desired for the spectrum sharing [15]. This research problem is extended to CE Multi-Carrier modulation waveforms [16], [17] and CE-OFDM waveforms [18]. These waveforms can be extended to CE-BPSK waveforms [19] and CE-QPSK waveforms [20]. CE Waveforms need to have FACE property, such that to have equal power for all transmit antenna elements. New waveforms are designed based on finite alphabet considering CE-BPSK and CE-QPSK spectrum sharing constraint [21], [22] and [23]. The work is based on static and time varying interference channels and proved zero interference between radar and communication system. However, this results in loss in the radar performance as the beamforming is no more optimal for target estimation and detection. Performance tradeoff between radar-communications can be gained by relaxing the zero-forcing precoder to restrict controllable interference levels on the communication system [24], which guarantees a high realistic co-existence approach. Another approach is the usage of relays between the primary user and secondary user, which is an active research area in the cognitive area network. Relays are used to sense the primary user signal and then allow the secondary user to do spectrum sharing. The performance is analyzed through the SNR and probability of detection as before for both primary user and secondary user through Rayleigh fading channels [25], [26].

Researchers in [27], has utilized optimization methods to perceive Communication Radar Spectrum Sharing(CRSS). To increase the Signal-to-Interference-plus-Noise-Ratio (SINR) of the radar, a joint design of communication covariance matrix and radar beamforming is discussed keeping capacity and power constraints for communication's side. Identical work has been adopted for co-existence among the point-to-point MIMO communication system and MIMO-matrix completion radar [28], [29], keeping radar sub sampling matrix as the optimization variable. For practical coexistence concern, assumptions on vigorous beamforming design with inferior Channel State Information (CSI) on the communication side, where the probability of detection of radar is increased subject to the constraint on SINR of the users in downlink and the Base Station (BS) power budget [30]. Further enhancement of the method is carried out, in which innovative beamforming design has been shown in [31], where the interference is exploited as meaningful power source. It shows power savings magnitude. All above mentioned approaches of coexistence are well generated, but a major problem is the communication devices and the radar need to transfer side information to study radar waveforms, CSI and formats of communication modulation. Practically, side information is retrieved from the backhaul system, but it is difficult to implement a complicated system [29]. A novel architecture is proposed for ensuring the power budget and the SINR of the communication applications for the transmitted beamforming methods of the merged Radar Communication (RadCom) systems. Using shared and separate models for the radar and communication systems, weighted optimization is used for keeping SINR as constraint as a penalty term in the objective function. Through weighted optimization, performance is matched with the original beamforming design with lower complexity [32], [33]. The work done by [32] is extended and a new algorithm is proposed for a MIMO radar communication dual function in [34] for concurrent detection of target and down link communication between the systems. Single transmitter with multiple antennas having multiple down link cellular users are considered, which detect targets in parallel. Dual methods are designed for waveforms with respect to total and pre-antenna power optimization constraints based on branch and bound framework is used. The work done has a tradeoff between performance of radar and communication system.

On the other hand, different algorithms are discussed to comprehend a given covariance matrix based on different constraints to solve beam pattern matching problem for MIMO radars and MIMO communication systems. For optimizing the problem of beam pattern, the waveforms using an arbitrary cross correlation matrix have been suggested in [35].

They showed their work for constant modulus constraint. [36] worked on waveforms focussing on total power as a constraint over a function of least square. The waveforms based on omnidirectional beam pattern and antenna lobes with specific threshold values are suggested in [37]. Waveforms focussing on ripple energy, and bandwidth is done in [38]. Synthesis of antenna array via flat top patterns using random drift particles swarm optimization techniques have been implemented in [39].

All these works did not consider FACE property. BPSK waveforms with FACE property have been suggested in [19]. QPSK waveforms with FACE property have also been shown. However, the suggestion of using QPSK waveforms does not satisfy FACE property. A mathematical model for the creation of the desired covariance matrix of QPSK waveform with FACE property has been suggested in [20]. The mathematical proof and implementation through the algorithms to create a covariance matrix with FACE property have been implemented in [23]. Constant modulus work is done by [15], working on waveform design for target detection as well as for cellular transmission. This approach is carried for minimizing the download multi-user interference as well as for the non-orthogonality of the transmitted waveform. They have solved the optimization through singular value decomposition and by Riemannian conjugate gradient algorithm. The work is extended to Dual Functional Radar Communication (DFRC) systems, which are used in millimeter-wave band using the Hybrid Analog Digital (HAD) beam forming technique [40].

Transmit beamforming with spectrum sharing along with FACE property is a contemporary research problem. BPSK and QPSK waveforms under the spectrum sharing constraint have been presented in [20]. They showed the spectrum sharing scenario for radar with a communication system over a single channel. They also showed that the waveforms are designed in such a way that they do not interfere with each other. The approach to multiple channels for MIMO radar and MIMO communication system has been extended in [22], [23]. The above works have considered and formulated waveforms using a single angle only.

### A. CONTRIBUTION

The work in this paper is an entension based on [14]. The additional elevation angle is added with the existing azimuth angle. With this addition, the target can be located with respect to two dimensions, i.e., with respect to azimuth angle and elevation angle. With the addition of elevation angle, the radar can detect the target in the air with certain probability "$p$" while previously the radar can detect an object on the ground plane under spectrum sharing constraints.

The covariance matrix is created using BPSK beam pattern designed based FACE property using two angles. Along with this, it is proved that the BPSK covariance matrix is positive semi-definite. The waveforms are designed in such a manner that the constrained optimization problem is converted to unconstrained optimization problem. Also, the radar shares the available spectrum with the cellular system through different relaying protocols and guarantees that the cellular system experiences zero interference. The design is based on a static interference channel. The work is considered for the case of stationary maritime with MIMO radars where the interference channel is slow moving or almost stationary.

**TABLE 1. Table for notations used in this paper.**

| Notation | Description |
|---|---|
| $\widetilde{\mathbf{x}}(n)$ | BPSK Transmitted Radar Waveform |
| $\mathbf{a}(\theta,\phi)_k$ | Steering vector to steer signal to target angle $(\theta,\phi)_k$ |
| $\widetilde{\mathbf{r}}_k(n)$ | Received radar waveform from target at $(\theta,\phi)_k$ |
| $\widetilde{\mathbf{R}}$ | Correlation matrix of BPSK waveforms |
| $\mathcal{L}_i$ | Total number of user equipments (UEs) in the $i^{\text{th}}$ cell |
| $\mathcal{K}$ | Total Number of BSs |
| $M$ | T/R Radar Antennas |
| $N_{\text{BS}}$ | T/R BS antennas |
| $\mathbf{H}_i$ | $i^{\text{th}}$ interference channel |
| $H_n$ | Hermite Polynomial |
| $\mathbf{y}_i(n)$ | Signal Received at the $i^{\text{th}}$ BS |
| $\mathbf{P}_i$ | Projection matrix |
| $\odot$ | Hadamard Product |
| $Vec$ | Operator that stores the column of a matrix in one column vector |

Table 1 shows the summary of notations used in this paper. The rest of the paper is organized as follows: Section II describes the system model, Section III describes simulation setup and in Section IV, the paper is concluded.

## II. SYSTEM MODEL

### A. WAVEFORM DESIGN FOR RADAR IN COEXISTENCE WITH CELLULAR COMMUNICATION SYSTEM

In this section, architecture for the spectrum sharing and waveform design with an algorithm for the 3 GHz band is discussed. The spectrum is shared by the radar and cellular system through different relay systems. Fading effect is reduced due to the cooperative communication amongst MIMO radar and communication systems, making the network more reliable. Different two-hop and three-hop relaying protocols are used to achieve cooperative diversity.

Figure 1 below shows the co-existence scenario of static MIMO radar and cellular systems through different two-hop relaying protocols. The radar is considered on top of the static ship, keeping channel to be static. Relays are placed at the edge of the range of radar, to detect the energy signal of the radar (presence of the primary/radar signal), which is calculated through Signal to Noise Ratio (SNR). Specific threshold "$\gamma$" is set for sharing spectrum between two systems. If the energy calculated is lower than the threshold, the relay will not allow communication system for the spectrum sharing. Projection of signal is done through the Singular Value Decomposition (SVD), which is performed after the SNR is above the threshold level. Whereas, Figure 2 below shows three-hop relaying protocol for the co-existence scenario of static MIMO radar and MIMO cellular system.

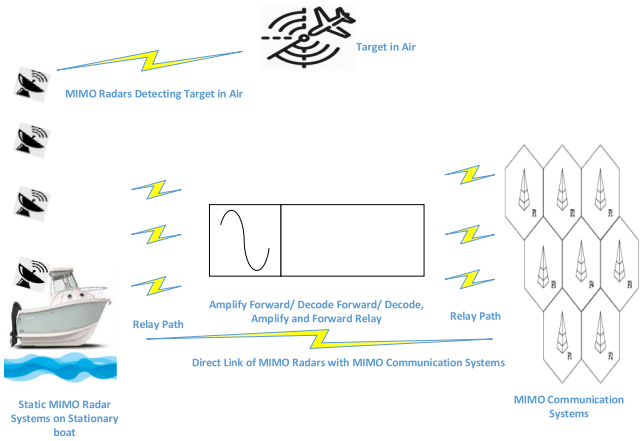


**FIGURE 1.** Spectrum sharing scenario between MIMO radar and MIMO communication through 2-Hop AF/DF/DAF relaying system.

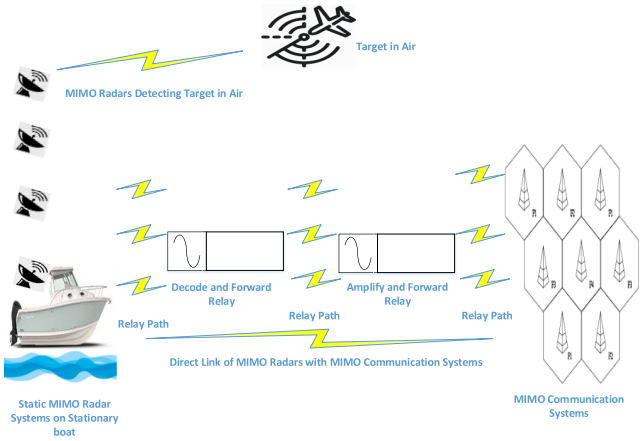


**FIGURE 2.** Spectrum sharing scenario between MIMO radar and MIMO communication through 3-Hop relaying system.

In both cases, the radar needs to detect the target and also share ⟩ interference channels with the communication system.

Waveform design for MIMO radar targeting $K$ number of targets in air is considered. Since, collocated antennas give better performance in terms of target parameter estimation, Therefore, two orthogonal Uniform Linear Arrays (ULA), each having $M$ transmit and receive collocated antennas are used.

Now considering MIMO communication system, which has $\mathcal{K}$ base stations, each having $N_{\text{BS}}$ antennas. The $i^{\text{th}}$ Base Station (BS) supports $\mathcal{L}_i$ user equipment's (UEs). The signal received at the $i^{\text{th}}$ base station is given in equation (1) as,

$$\mathbf{y}_i(n) = \sum_j H_{i,j}\,\widetilde{\mathbf{x}}(n) + \mathbf{w}(n) \quad \text{for } 1 \le i \le \mathcal{K} \text{ and } 1 \le j \le \mathcal{L}_i \tag{1}$$

where $\mathbf{y}_i(n)$ is the estimated signal at the receiver.

Where $\mathbf{H}_{i,j}$ is defined as the channel matrix, and $\mathbf{w}(n)$ is the additive white Gaussian noise. Since the spectrum is shared between radar and cellular system; therefore defining the $i^{\text{th}}$ interference channel between radar and on a cellular system as shown in equation (2),

$$\mathbf{H}_i \triangleq \begin{bmatrix} h_i^{(1,1)} & \cdots & h_i^{(1,M)} \\ \vdots & \ddots & \vdots \\ h_i^{(N_{\text{BS}},1)} & \cdots & h_i^{(N_{\text{BS}},M)} \end{bmatrix} \quad (N_{\text{BS}} \times M) \tag{2}$$

where $i = 1, 2, \ldots, \mathcal{K}$, and $h_i^{(m,k)}$ represents the channel coefficients from the $m^{\text{th}}$ antenna element of the $i^{\text{th}}$ BS to the $k^{\text{th}}$ antenna element of MIMO radar. The Rayleigh probability density function of the interference channel $H_i$ is given as,

$$f(h \mid \rho) = \frac{h}{\rho^2} e^{\frac{-h^2}{2\rho^2}} \tag{3}$$

where $\rho$ is the mode of the Rayleigh distribution.

### 1) AMPLIFY AND FORWARD RELAYING PROTOCOL

Considering the Amplify and Forward (AF) relaying protocol shown in Figure 1, the signal received from the primary source radar to relay, is amplified only and forwarded to the secondary source communication system. The relay does not regenerate the signal. Noise added in the channel is also amplified during amplification process and forwarded to the destination. This technique is called as a non-regenerative relaying protocol. The amplified signal "$x_r(n)$" from the AF relay to the communication system is written as,

$$x_r(n) = x_t(n) \cdot \beta \tag{4}$$

where "$x_t(n)$" is received signal from transmitted radar signal and scaling factor "$\beta$" is given as,

$$\beta = \sqrt{\frac{P_t}{P_r|h|^2 + \sigma^2}} \tag{5}$$

where "$P_t$" is the radar power, "$P_r$" is the relay power, "$\sigma^2$" is the variance of noise and "$h$" defines coefficient between relay and radar.

### 2) DECODE AND FORWARD RELAYING PROTOCOL

For the case of Decode and Forward (DF) relaying protocol shown in Figure 1, the signal is decoded first and then forwarded to the destination. The regenerated signal is approximate of the transmitted signal. The forwarded signal "$x_{r,s}(n)$" from the relay to the destination is given as,

$$x_{r,s}(n) = \sqrt{\frac{P_r}{P_t}}\tilde{x}_t(n) \tag{6}$$

where as "$\tilde{x}_t(n)$" is the decoded (estimated) signal.

### 3) DECODE, AMPLIFY AND FORWARD RELAYING PROTOCOL

Considering Decode, Amplify and Forward (DAF) relaying protocol shown in Figure 1, the data is first decoded and then amplified. The destination gets the amplified signal. The forwarded signal from the DAF relay to the destination is given as,

$$x_{r,d}(n) = x_{r,s}(n) \cdot \beta \tag{7}$$

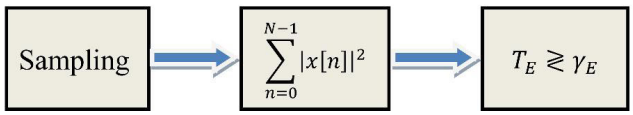


**FIGURE 3.** Energy detection method.

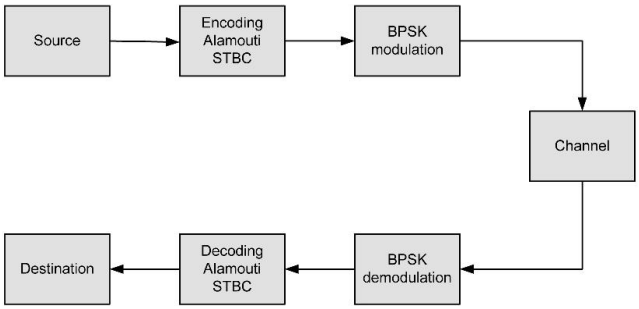


**FIGURE 4.** System-model.

where "$x_{r,s}(n)$" is the decode and forward equation, which is multiplied by scaling factor "$\beta$". The radar waveform is designed in such a way that it is in the null space of the channel matrix, i.e., $\mathbf{H}_i\widetilde{\mathbf{x}}(n) = \mathbf{0}$. A projection matrix is designed which satisfies the condition $\mathbf{H}_i\widetilde{\mathbf{x}}(n) = \mathbf{0}$. In this paper, for sharing of spectrum, the projection is based on the energy detection method. The energy is detected from an energy detector for a specific time period to measure the presence or absence of the radar signal, which is considered as the primary user. The detection is based on a specific defined threshold level. Figure 3 shows the mechanism for the detection of the radar's signal. Figure 4 shows the system model for the encoding and decoding of the Alamouti coding scheme.

The projection matrix is expressed as in equation (8)

$$\mathbf{P}_i \triangleq \mathbf{V}_i\widetilde{\mathbf{\Sigma}}_i'\mathbf{V}_i^H. \tag{8}$$

Figure 5 shows a conceptual view of the target detection at the location $(\theta, \phi)_k$. The target can be located from two directions, i-e., through azimuth angle and elevation angle. After discussing the co-existence scenario, we now formulate the waveform design.

### B. FACE BEAMPATTERN DESIGN FOR TARGET DETECTION

In this paper, BPSK waveforms have been designed which have FACE property that can detect a target in both azimuth and elevation plane. $M$ transmit antennas are selected in a linear array with half-wavelength spacing. The transmitted BPSK signal from the antenna is given as,

$$\widetilde{\mathbf{x}}(n) = \begin{bmatrix}\widetilde{x}_1(n) & \widetilde{x}_2(n) & \cdots & \widetilde{x}_m(n)\end{bmatrix}^T \tag{9}$$

where $\widetilde{x}_(n)$ is a BPSK signal and $m^{\text{th}}$ represents the transmit element at time index $n$. Assuming the target $K$ at location $(\theta, \phi)_k$, the signal received from the target is given as,

$$\widetilde{r}_k(n) = \mathbf{a}^H(\theta, \phi)_k\widetilde{\mathbf{x}}(n) \tag{10}$$

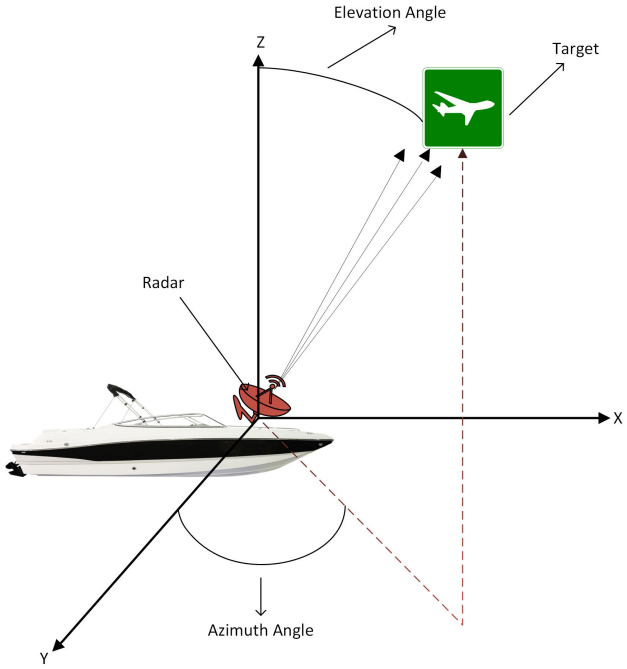


**FIGURE 5.** Target detection in spherical coordinate system.

where $\mathbf{a}(\theta, \phi)_k$ is the steering vector for the azimuth angle $(\theta)$ and elevation angle $(\phi)$ and is defined as

$$a(\theta, \phi)_k = vec\Big(Z_k \odot \big[u(\theta, \phi)v^T(\theta, \phi)\big]\Big) \tag{11}$$

$Z_k$ is the matrix of 1's of dimension $M \times N$. $M$ represents transmit radar antenna elements and $N$ represents receive radar antenna elements.

$$u(\theta, \phi) \in C^{M\times 1}$$
$$v(\theta, \phi) \in C^{N\times 1}$$

where

$$\mathbf{u}(\theta, \phi)_k = \begin{bmatrix}1 & e^{j2\pi d_m \sin\theta_k \cos\phi_k} & \cdots & e^{j2\pi(M-1)d_m \sin\theta_k \cos\phi_k}\end{bmatrix}^T \tag{12}$$

and

$$\mathbf{v}(\theta, \phi)_k = \begin{bmatrix}1 & e^{j2\pi d_n \sin\theta_k \sin\phi_k} & \cdots & e^{j2\pi(N-1)d_n \sin\theta_k \sin\phi_k}\end{bmatrix}^T \tag{13}$$

The actual received power for the target $K$ at $(\theta, \phi)_k$ location is as follows,

$$\begin{aligned} P(\theta, \phi)_k &= \mathbb{E}\{\mathbf{a}^H(\theta, \phi)_k\,\widetilde{\mathbf{x}}(n)\,\widetilde{\mathbf{x}}^H(n)\,\mathbf{a}(\theta, \phi)_k\} \\ &= \mathbf{a}^H(\theta, \phi)_k\,\widetilde{\mathbf{R}}\,\mathbf{a}(\theta, \phi)_k \end{aligned} \tag{14}$$

Using cost function expressed in 15, the required BPSK waveform $\varphi(\theta, \phi)_k$ is generated by reducing the square of the error between $P(\theta, \phi)_k$ and $\varphi(\theta, \phi)_k$.

$$J(\widetilde{\mathbf{R}}) = \frac{1}{K}\sum_{k=1}^{K}\Big(\mathbf{a}^H(\theta, \phi)_k\,\widetilde{\mathbf{R}}\,\mathbf{a}(\theta, \phi)_k - \varphi(\theta, \phi)_k\Big)^2 \tag{15}$$

where $\widetilde{\mathbf{R}}$ is the transmitted signal covariance matrix which should be positive semi-definite. Also, for constant envelop property, all antennas must have same transmit power. The optimization problem shown in equation (15) has constraints; therefore, it can not be chosen freely. The constraints are as,

$$C_1 : \mathbf{v}^H \widetilde{\mathbf{R}} \mathbf{v} \geq 0, \quad \forall\, \mathbf{v},$$
$$C_2 : \widetilde{\mathbf{R}}(i,i) = constant, \quad i = 1, 2, \ldots, M,$$

Positive semi-definite constraint is fulfilled by $C_1$ and constant envelop constraint is fulfilled by $C_2$. Writing the optimization problem with constraints as,

$$\min_{\widetilde{\mathbf{R}}} \frac{1}{K} \sum_{k=1}^{K} \left( \mathbf{a}^H(\theta,\phi)_k \, \widetilde{\mathbf{R}} \, \mathbf{a}(\theta,\phi)_k - \varphi(\theta,\phi)_k \right)^2$$
$$\text{subject to } \mathbf{v}^H \widetilde{\mathbf{R}} \mathbf{v} \geq 0, \quad \forall\, \mathbf{v},$$
$$\widetilde{\mathbf{R}}(i,i) = constant, \quad i = 1, 2, \ldots, M. \tag{16}$$

It is possible to transfer the non-linear optimization problem with constraints to an optimization without constraints. The waveform matrix $\widetilde{\mathbf{X}}$ in equation (18) having $N$ samples is obtained by synthesizing $\widetilde{\mathbf{R}}$.

$$\widetilde{\mathbf{X}} = \begin{bmatrix} \widetilde{\mathbf{x}}(1) & \widetilde{\mathbf{x}}(2) & \cdots & \widetilde{\mathbf{x}}(N) \end{bmatrix}^T. \tag{17}$$

This can be grasped as,

$$\widetilde{\mathbf{X}} = \boldsymbol{\mathcal{X}} \boldsymbol{\Lambda}^{1/2} \mathbf{W}^H \tag{18}$$

where $\boldsymbol{\Lambda}$ and $\mathbf{W}$ are matrices containing eigenvalues and eigenvectors respectively, while $\boldsymbol{\mathcal{X}}$ represents a zero mean and unit variance matrix.

### C. FACE BASED BPSK WAVEFORMS FOR TARGET DETECTION

Considering real Gaussian Random Variable (RV) $\widetilde{x}_m$ with zero mean and unit variance, which is mapped to a BPSK RV $\widetilde{z}_m$ as in equation 19,

$$\widetilde{z}_m = \frac{1}{\sqrt{2}} \left[ \text{sign}(\widetilde{x}_m) \right]. \tag{19}$$

Equation (20) describes the $(p, q)$th element of the gaussian RV,

$$\mathbb{E}\{\widetilde{z}_p \widetilde{z}_q\} = \gamma_{pq} = \gamma_{\Re_{pq}} \tag{20}$$

where $\gamma_{\Re_{pq}}$ are the real parts of $\gamma_{pq}$. If, Gaussian RVs $\widetilde{x}_p, \widetilde{x}_q$, are chosen correctly, then

$$\gamma_{\Re_{pq}} = \mathbb{E}\left\{ \text{sign}(\widetilde{x}_p) \text{sign}(\widetilde{x}_q) \right\} \tag{21}$$

The real $(p, q)^{th}$ Gaussian random variable is stated in equation (22) as,

$$\mathbb{E}\{\widetilde{z}_p \widetilde{z}_q\} = \frac{2}{\pi} \left[ \sin^{-1} \left( \mathbb{E}\{\widetilde{x}_p \widetilde{x}_q\} \right) \right]. \tag{22}$$

The real Gaussian covariance matrix $\widetilde{\mathbf{R}}_g$ is stated as,

$$\widetilde{\mathbf{R}}_g \triangleq \Re(\mathbf{R}_g) \tag{23}$$

where $\Re(\mathbf{R}_g)$ is real Gaussian convariance matrix, therefore we can write equation (23) as,

$$\widetilde{\mathbf{R}} = \frac{2}{\pi} \left[ \sin^{-1} \left( \Re(\mathbf{R}_g) \right) \right]. \tag{24}$$

A real Gaussian covariance matrix is obtained through $\widetilde{\mathbf{R}}_g = \widetilde{\mathbf{U}}^H \widetilde{\mathbf{U}}$ transform. Equation (29) represents $\widetilde{\mathbf{U}}$. Real component of $\widetilde{\mathbf{U}}$ is written as,

$$\widetilde{\mathbf{U}} = \Re(\widetilde{\mathbf{U}}) \tag{25}$$

where $\Re(\widetilde{\mathbf{U}})$ is given by equation (32). Alternately, $\widetilde{\mathbf{R}}_g$ can also be expressed as,

$$\widetilde{\mathbf{R}}_g = \left[ \Re(\widetilde{\mathbf{U}})^H \Re(\widetilde{\mathbf{U}}) \right]. \tag{26}$$

$$\Re\left(\widetilde{\mathbf{U}}\right) = \Re\left(\widehat{U}\right) \cdot \Re\left(\overline{U}\right) \tag{32}$$

### D. COVARIANCE/CORRELATION MATRIX SYNTHESIS FOR DESIRED BPSK BEAMPATTERN

In this section, it is proved that the covariance matrix $\widetilde{\mathbf{R}}_g$ can be used to design the desired BPSK beampattern and $M$ BPSK waveforms are generated with finite alphabet constant envelop property. The real component of BPSK RV can be shown in equation (33).

$$\widetilde{\mathbf{R}} = \frac{2}{\pi} \left[ \sin^{-1} \left( \Re(\mathbf{R}_g) \right) \right]. \tag{33}$$

Through equation (16), the optimization problem can be rewritten using equation (33) in (34), as shown at the bottom of the next page.

In this paper, $\widetilde{\mathbf{U}}$ and $\widetilde{\mathbf{R}}_g$ are functions of "$\boldsymbol{\varsigma}$" and "$\varrho$", which are the unknown variables of $(\theta)$ and $(\phi)$. Equation (35) and (36) shows alternate form of cost function,

$$\boldsymbol{\varsigma} = \begin{bmatrix} \boldsymbol{\zeta}^T & \widetilde{\boldsymbol{\zeta}}^T & \alpha \end{bmatrix}^T, \tag{35}$$

and

$$\begin{aligned} \boldsymbol{\zeta}^T &= \begin{bmatrix} \zeta_{21} & \zeta_{21} & \cdots & \zeta_{21} \end{bmatrix}^T, \\ \widetilde{\boldsymbol{\zeta}}^T &= \begin{bmatrix} \zeta_1 & \zeta_2 & \cdots & \zeta_M \end{bmatrix}^T. \\ \boldsymbol{\varrho} &\begin{bmatrix} \boldsymbol{\xi}^T & \widetilde{\boldsymbol{\xi}}^T & \alpha \end{bmatrix}^T, \\ \boldsymbol{\xi}^T &= \begin{bmatrix} \xi_{21} & \xi_{21} & \cdots & \xi_{21} \end{bmatrix}^T, \\ \widetilde{\boldsymbol{\xi}}^T &= \begin{bmatrix} \xi_1 & \xi_2 & \cdots & \xi_M \end{bmatrix}^T. \end{aligned} \tag{36}$$

Writing equation (35) and equation (36) as a cost function for equation (34) as,

$$J(\boldsymbol{\varsigma}) = \frac{1}{K} \sum_{k=1}^{K} \left[ \frac{2}{\pi} \mathbf{u}^H(\theta,\phi)_k \sin^{-1} \left( \Re(\mathbf{R}_g) \right) \mathbf{u}(\theta,\phi)_k - \alpha \varphi(\theta,\phi)_k \right]^2. \tag{37}$$

$$J(\boldsymbol{\varrho}) = \frac{1}{K} \sum_{k=1}^{K} \left[ \frac{2}{\pi} \mathbf{v}^H(\theta,\phi)_k \sin^{-1} \left( \Re(\mathbf{R}_g) \right) \mathbf{v}(\theta,\phi)_k - \alpha \varphi(\theta,\phi)_k \right]^2. \tag{38}$$

Using value of $\widetilde{\mathbf{R}}_g$ from equation (26) and rewriting equations (37) and (38) as,

$$J(\boldsymbol{\varsigma}) = \frac{1}{K}\sum_{k=1}^{K}\left[\frac{2}{\pi}\mathbf{u}^H(\theta,\phi)_k \sin^{-1}\left(\Re(\widetilde{\mathbf{U}})^H\Re(\widetilde{\mathbf{U}})\right) \times\mathbf{u}(\theta,\phi)_k - \alpha\varphi(\theta,\phi)_k\right]^2 \tag{39}$$

$$J(\boldsymbol{\varrho}) = \frac{1}{K}\sum_{k=1}^{K}\left[\frac{2}{\pi}\mathbf{v}^H(\theta,\phi)_k \sin^{-1}\left(\Re(\widetilde{\mathbf{U}})^H\Re(\widetilde{\mathbf{U}})\right) \times\mathbf{v}(\theta,\phi)_k - \alpha\varphi(\theta,\phi)_k\right]^2 \tag{40}$$

For the unknown parameters shown in equation (35), the partial derivative of $J(\boldsymbol{\zeta})$ with respect to $\zeta_{mn}$ can be found as,

$$\frac{\partial J(\boldsymbol{\varsigma})}{\partial\zeta_{mn}} = \left[\frac{2}{K}\sum_{k=1}^{K}\left\{\frac{2}{\pi}\mathbf{u}^H(\theta,\phi)_k \sin^{-1}\left(\Re(\mathbf{R}_g)\right)\mathbf{u}(\theta,\phi)_k - \alpha\varphi(\theta,\phi)_k\right\}\right] \times\left[\frac{\partial}{\partial\zeta_{mn}}\left\{\frac{2}{\pi}\mathbf{u}^H(\theta,\phi)_k \sin^{-1}\left(\Re(\mathbf{R}_g)\right) \times\mathbf{u}(\theta,\phi)_k\right\}\right] \tag{41}$$

$$\widehat{U} = \begin{pmatrix} e^{j\zeta_1} & e^{j\zeta_2}\sin(\zeta_{21}) & e^{j\zeta_3}\sin(\zeta_{31})\sin(\zeta_{32}) & \cdots & e^{j\zeta_M}\prod_{m=1}^{M-1}\sin(\zeta_{Mm}) \\ 0 & e^{j\zeta_2}\cos(\zeta_{21}) & e^{j\zeta_3}\sin(\zeta_{31})\cos(\zeta_{32}) & \cdots & e^{j\zeta_M}\prod_{m=1}^{M-2}\sin(\zeta_{Mm})\cos(\zeta_{M,M-1}) \\ 0 & 0 & e^{j\zeta_3}\cos(\zeta_{31}) & \ddots & \vdots \\ \vdots & \vdots & \ddots & \cdots & e^{j\zeta_M}\sin(\zeta_{M1})\cos(\zeta_{M2}) \\ 0 & 0 & \cdots & \cdots & e^{j\zeta_M}\cos(\zeta_{M1}) \end{pmatrix} \tag{27}$$

$$\overline{U} = \begin{pmatrix} e^{j\xi_1} & e^{j\xi_2}\sin(\xi_{21}) & e^{j\xi_3}\sin(\xi_{31})\sin(\xi_{32}) & \cdots & e^{j\xi_M}\prod_{m=1}^{M-1}\sin(\xi_{Mm}) \\ 0 & e^{j\xi_2}\cos(\xi_{21}) & e^{j\xi_3}\sin(\xi_{31})\cos(\xi_{32}) & \cdots & e^{j\xi_M}\prod_{m=1}^{M-2}\sin(\xi_{Mm})\cos(\xi_{M,M-1}) \\ 0 & 0 & e^{j\xi_3}\cos(\xi_{31}) & \ddots & \vdots \\ \vdots & \vdots & \ddots & \cdots & e^{j\xi_M}\sin(\xi_{M1})\cos(\xi_{M2}) \\ 0 & 0 & \cdots & \cdots & e^{j\zeta_M}\cos(\xi_{M1}) \end{pmatrix} \tag{28}$$

$$\widetilde{\mathbf{U}} = \widehat{U}\cdot\overline{U} \tag{29}$$

$$\Re\left(\widehat{U}\right) = \begin{pmatrix} \cos(\zeta_1) & \cos(\zeta_2)\sin(\zeta_{21}) & \cos(\zeta_3)\sin(\zeta_{31})\sin(\zeta_{32}) & \cdots & \cos(\zeta_M)\prod_{m=1}^{M-1}\sin(\zeta_{Mm}) \\ 0 & \cos(\zeta_2)\cos(\zeta_{21}) & \cos(\zeta_3)\sin(\zeta_{31})\cos(\zeta_{32}) & \cdots & \cos(\zeta_M)\prod_{m=1}^{M-2}\sin(\zeta_{Mm})\cos(\zeta_{M,M-1}) \\ 0 & 0 & \cos(\zeta_3)\cos(\zeta_{31}) & \ddots & \vdots \\ \vdots & \vdots & \ddots & \cdots & \cos(\zeta_M)\sin(\zeta_{M1})\cos(\zeta_{M2}) \\ 0 & 0 & \cdots & \cdots & \cos(\zeta_M)\cos(\zeta_{M1}) \end{pmatrix} \tag{30}$$

$$\Re\left(\overline{U}\right) = \begin{pmatrix} \cos(\xi_1) & \cos(\xi_2)\sin(\xi_{21}) & \cos(\xi_3)\sin(\xi_{31})\sin(\xi_{32}) & \cdots & \cos(\xi_M)\prod_{m=1}^{M-1}\sin(\xi_{Mm}) \\ 0 & \cos(\xi_2)\cos(\xi_{21}) & \cos(\xi_3)\sin(\xi_{31})\cos(\xi_{32}) & \cdots & \cos(\xi_M)\prod_{m=1}^{M-2}\sin(\xi_{Mm})\cos(\xi_{M,M-1}) \\ 0 & 0 & \cos(\xi_3)\cos(\xi_{31}) & \ddots & \vdots \\ \vdots & \vdots & \ddots & \cdots & \cos(\xi_M)\sin(\xi_{M1})\cos(\xi_{M2}) \\ 0 & 0 & \cdots & \cdots & \cos(\xi_M)\cos(\xi_{M1}) \end{pmatrix} \tag{31}$$

$$\begin{aligned} &\min_{\widetilde{\mathbf{R}}} \frac{1}{K}\sum_{k=1}^{K}\left[\frac{2}{\pi}\mathbf{a}^H(\theta,\phi)_k\left\{\sin^{-1}\left(\Re(\mathbf{R}_g)\right)\right\}\mathbf{a}(\theta,\phi)_k - \varphi(\theta,\phi)_k\right]^2 \\ &\text{subject to}\quad \mathbf{v}^H\widetilde{\mathbf{R}}\mathbf{v}\geq 0, \quad \forall\,\mathbf{v}, \\ &\qquad\qquad \widetilde{\mathbf{R}}(i,i) = constant, \quad i = 1,2,\ldots,M. \end{aligned} \tag{34}$$

Now, taking the partial derivative of $J(\boldsymbol{\zeta})$ with respect to $\zeta_l$ can be found as,

$$\frac{\partial J(\boldsymbol{\zeta})}{\partial \zeta_l} = \left[\frac{2}{K}\sum_{k=1}^{K}\left\{\frac{2}{\pi}\mathbf{u}^H(\theta,\phi)_k \sin^{-1}\left(\Re(\mathbf{R}_g)\right)\mathbf{u}(\theta,\phi)_k - \alpha\varphi(\theta,\phi)_k\right\}\right] \times \left[\frac{\partial}{\partial \zeta_l}\left\{\frac{2}{\pi}\mathbf{u}^H(\theta,\phi)_k \sin^{-1}\left(\Re(\mathbf{R}_g)\right) \times \mathbf{u}(\theta,\phi)_k\right\}\right] \tag{42}$$

Again, taking the partial derivative of $J(\boldsymbol{\zeta})$ with respect to $\alpha$, which can be found as,

$$\frac{\partial J(\boldsymbol{\zeta})}{\partial \alpha} = \frac{-2\varphi(\theta,\phi)_k}{K}\left[\sum_{k=1}^{K}\left\{\frac{2}{\pi}\mathbf{u}^H(\theta,\phi)_k \sin^{-1}\left(\Re(\mathbf{R}_g)\right) \times \mathbf{u}(\theta,\phi)_k - \alpha\varphi(\theta,\phi)_k\right\}\right] \tag{43}$$

Similarly, the partial derivative of $J(\boldsymbol{\varrho})$ with respect to any element of $\boldsymbol{\xi}$,i.e. $\xi_{mn}$, can be obtained as,

$$\frac{\partial J(\boldsymbol{\varrho})}{\partial \xi_{mn}} = \left[\frac{2}{K}\sum_{k=1}^{K}\left\{\frac{2}{\pi}\mathbf{v}^H(\theta,\phi)_k \sin^{-1}\left(\Re(\mathbf{R}_g)\right)\mathbf{v}(\theta,\phi)_k - \alpha\varphi(\theta,\phi)_k\right\}\right] \times \left[\frac{\partial}{\partial \xi_{mn}}\left\{\frac{2}{\pi}\mathbf{v}^H(\theta,\phi)_k \sin^{-1}\left(\Re(\mathbf{R}_g)\right) \times \mathbf{v}(\theta,\phi)_k\right\}\right] \tag{44}$$

The partial derivative of $J(\boldsymbol{\varrho})$ with respect to any element of $\widetilde{\boldsymbol{\xi}}$, say $\xi_l$, can be obtained as,

$$\frac{\partial J(\boldsymbol{\varrho})}{\partial \xi_l} = \left[\frac{2}{K}\sum_{k=1}^{K}\left\{\frac{2}{\pi}\mathbf{v}^H(\theta,\phi)_k \sin^{-1}\left(\Re(\mathbf{R}_g)\right)\mathbf{v}(\theta,\phi)_k - \alpha\varphi(\theta,\phi)_k\right\}\right] \times \left[\frac{\partial}{\partial \xi_l}\left\{\frac{2}{\pi}\mathbf{v}^H(\theta,\phi)_k \sin^{-1}\left(\Re(\mathbf{R}_g)\right) \mathbf{v}(\theta,\phi)_k\right\}\right] \tag{45}$$

Lastly, the partial differentiation of $J(\boldsymbol{\varrho})$ with respect to $\alpha$ is,

$$\frac{\partial J(\boldsymbol{\varrho})}{\partial \alpha} = \frac{-2\varphi(\theta,\phi)_k}{K}\left[\sum_{k=1}^{K}\left\{\frac{2}{\pi}\mathbf{v}^H(\theta,\phi)_k \sin^{-1}\left(\Re(\mathbf{R}_g)\right) \times \mathbf{v}(\theta,\phi)_k - \alpha\varphi(\theta,\phi)_k\right\}\right] \tag{46}$$

### E. OPTIMUM NULL SPACE PROJECTION

For the design, beam pattern optimization problem is considered and FACE BPSK waveforms are designed in 2D with the addition of elevation angle. It is proven that such waveforms are positive semi-definite and have constant envelope. After waveform design for $K$ number of targets at the location $(\theta, \phi)$, new constraint of spectrum sharing is considered.

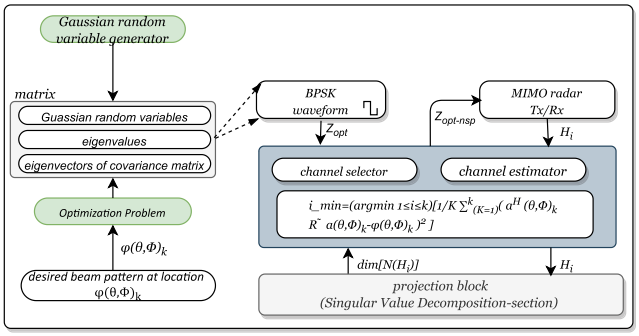


**FIGURE 6.** BPSK transmit beampattern design problem in spherical coordinate system.

The criteria for spectrum sharing is such that both systems do not interfere with each other. Consider the case of a ship docked at a harbour. Since the ship is stationary, therefore the radar which are mounted on ship is also stationary and interference channel is taken as stationary too. This optimization problem is formulated in equation (47), as shown at the bottom of the next page.

Figure 6 below shows the process of waveform design. Thus the optimum waveform is obtained as,

$$\breve{\widetilde{\mathbf{Z}}}_{\mathrm{NSP}}^{\mathrm{opt}} = \widetilde{\mathbf{Z}}_i^{\mathrm{opt}}\mathbf{P}_i^H. \tag{48}$$

The designed covariance matrix of the waveform is shown as,

$$\breve{\widetilde{\mathbf{R}}}_i = \frac{1}{N}\left(\breve{\widetilde{\mathbf{Z}}}_{\mathrm{NSP}}^{\mathrm{opt}}\right)^H \breve{\widetilde{\mathbf{Z}}}_{\mathrm{NSP}}^{\mathrm{opt}}. \tag{49}$$

It is suggested to select the convariance matrix $\breve{\widetilde{\mathbf{R}}}_i$ of the transmitted waveform in such a way that the design of the covariance matrix is very close to the desired covariance matrix, i.e.,

$$i_{\min} \triangleq \arg\min_{1\le i\le \mathcal{K}}\left[\frac{1}{K}\sum_{k=1}^{K}\left(\mathbf{a}^H(\theta,\phi)_k \breve{\widetilde{\mathbf{R}}}_i \mathbf{a}(\theta,\phi)_k - \varphi(\theta,\phi)_k\right)^2\right] \tag{50}$$

$$\widetilde{\mathbf{R}}_{\mathrm{NSP}}^{\mathrm{opt}} \triangleq \breve{\widetilde{\mathbf{R}}}_{i_{\min}}. \tag{51}$$

So it is suggested to select $\mathbf{P}_i$, which is designed to transmit maximum power at the target location $(\theta, \phi)$. Algorithm (1) shows the static constrained waveform design for MIMO radar.

## III. SIMULATION SETUP

For the design of constrained BPSK waveforms having FACE property, we used ten radar transmit and receive element arrays. Whereas, the number of communication receive elements are also ten. The inter-element spacing is taken as half-wavelength of the operating frequency. Since, the design is based on constant envelope, every antenna radiates unit power. The total symbols are taken as 5000. The beam pattern is designed for $(\theta, \phi)_k$. We performed 100 Monte Carlo trials of BPSK waveforms in $(\theta, \phi)_k$ direction and average our

**Algorithm 1** Static Constrained Waveform Design Algorithm for MIMO Radar

**loop**
  **for** $i = 1 : \mathcal{K}$ **do**
    Take Channel State Information of $\mathbf{H}_i$ via $i^{\text{th}}$ Base Station's feedback channel.
    Formulate projection matrix $\mathbf{P}_i$ based on Eq.(8)
    Design desired BPSK waveform $\widetilde{\mathbf{Z}}_i^{\text{opt}}$ using equation (47) as optimization problem
    Taking null space of $i^{\text{th}}$ interference channel through $\overset{\approx}{\mathbf{Z}}_{\text{NSP}}^{\text{opt}} = \widetilde{\mathbf{Z}}_i^{\text{opt}} \mathbf{P}_i^H$, Setup the BPSK waveform onto it.
  **end for**
  Find $i_{\min} =$
  $\arg\min_{1 \le i \le \mathcal{K}} \left[ \frac{1}{K} \sum_{k=1}^{K} \left( \mathbf{a}^H(\theta, \phi)_k \, \overset{\approx}{\mathbf{R}}_i \, \mathbf{a}(\theta, \phi)_k - \varphi(\theta, \phi)_k \right)^2 \right]$.
  Set $\widetilde{\mathbf{R}}_{\text{NSP}}^{\text{opt}} = \overset{\approx}{\mathbf{R}}_{i_{\min}}$ for the desired covariance matrix which is to be transmitted.
**end loop**

designed beam pattern. We generated a Rayleigh interference channel of dimension $N_{\text{BS}} \times M$ for each Monte Carlo trial. For spectrum sharing, we use different relaying protocols amongst MIMO radar and communication systems. We use energy detection mechanism for detecting the presence of the radar signal, which is the primary user (PU) and then allows the communication system, which is the secondary user (SU) to use the spectrum of PU. After this the null space is calculated, which is based on our algorithm 1. In the end, the optimization problem is solved for the stationary ship with MIMO radar system.

### A. WAVEFORM FOR RADAR

Transmit beam pattern for a stationary MIMO radar in $(\theta, \phi)_k$ direction are designed with having $K$ number of targets in the air. The desired beam pattern has two main lobes from $-55°$ to $-35°$ and from $35°$ to $55°$ in $(\theta_k)$ direction, whereas two main lobes $-40°$ to $-35°$ and from $35°$ to $40°$ in $(\phi_k)$ direction. BPSK transmit beam forming is performed by solving equation (47). Different threshold $(\sigma)$ levels are used to get the null space, so that communication system can share the spectrum with the radar system. Figure 5 shows the target at the location $(\theta, \phi)$, for which we designed the beam pattern at the desired location $(\theta, \phi)_k$. Figure 7 shows the desired beam pattern at $-55°$ to $-35°$ and from $35°$ to $55°$ in $(\theta_k)$ direction. The designed beam pattern is achieved by using threshold values set to 1, 2 and 3 used in algorithm 1. The designed beam pattern is close to the desired beam pattern.

Singular Value Decomposition (SVD) is computed, which is based on an algorithm (1). If no null space is available

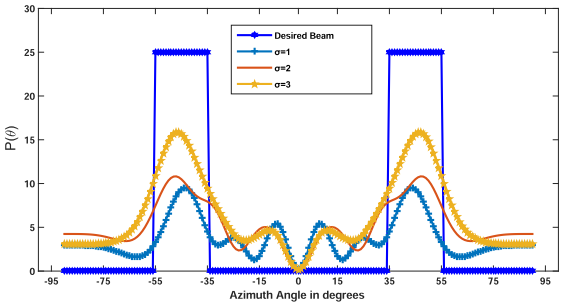


**FIGURE 7.** Azimuth angle desired waveform compared with designed waveform.

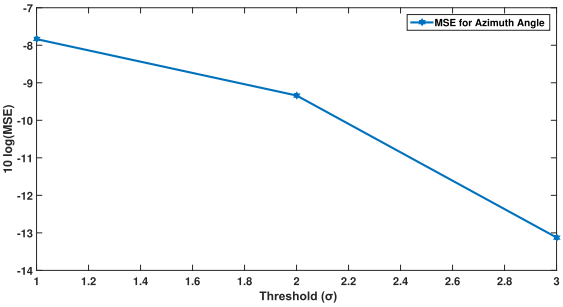


**FIGURE 8.** Minimum square error for azimuth angle.

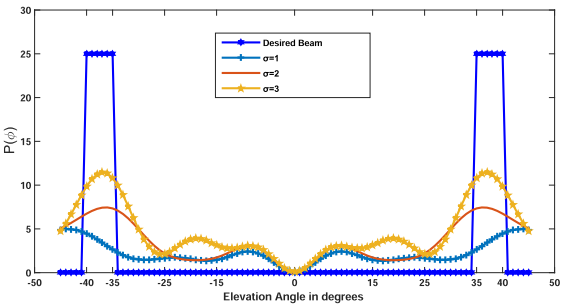


**FIGURE 9.** Elevation angle desired waveform compared with designed waveform.

for the spectrum sharing between radar and communication system, we assign different threshold $(\sigma)$ values for our spectrum sharing scenario so as to get null space required for the spectrum sharing. By setting threshold values, null spaces are obtained for the spectrum sharing. Figure 7 shows that the waveform design closely matches with the desired waveform. The higher the threshold, better the waveform design. There is a trade-off between designing waveform in the desired direction as well as spectrum sharing with the other system.

The lower threshold ($\sigma = 1$) has higher nulls and can share more bandwidth more as compared to the higher threshold ($\sigma = 3$). In general, we can say higher the nulls, higher the bandwidth for spectrum sharing, while lower the

$$\min_{\zeta_{ij}, \zeta_l, \xi_{ij}, \xi_l} \frac{1}{K} \sum_{k=1}^{K} \left[ \frac{2}{\pi} \mathbf{a}^H(\theta, \phi)_k \mathbf{P}_i \left\{ \sin^{-1} \left( \Re(\widetilde{\mathbf{U}})^H \Re(\widetilde{\mathbf{U}}) \right) \right\} \times \mathbf{P}_i^H \mathbf{a}(\theta, \phi)_k - \alpha \varphi(\theta, \phi)_k \right]^2 \tag{47}$$

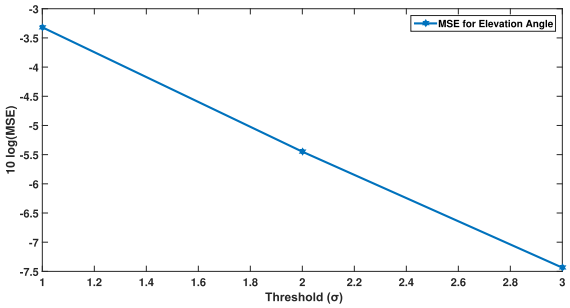


**FIGURE 10.** Minimum square error for elevation angle.

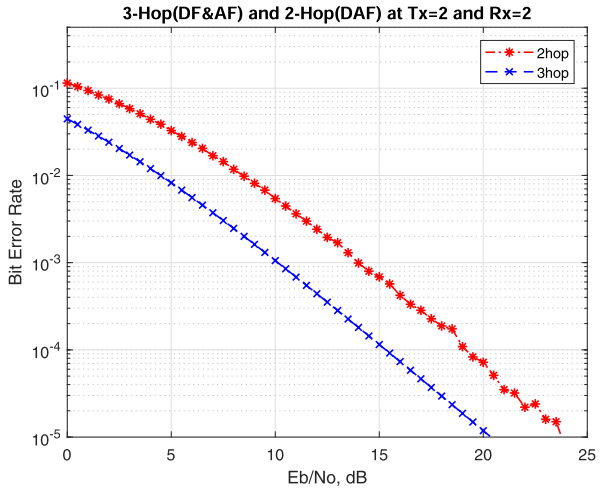


**FIGURE 11.** Performance evaluation of SNR versus BER for 2 and 3 hop relays system with Tx = 2 & Rx = 2.

nulls, less bandwidth is available of spectrum sharing. This clearly shows the basic requirement of spectrum sharing with minimum degradation to performance. Figure 8 shows the Minimum Square Error (MSE) between desired beam pattern at $-50°$ to $-30°$ and from 30° to 50° in ($\theta_k$) direction.

Figure 9 shows the desired beam pattern at $-40°$ to $-35°$ and from 35° to 40° in ($\phi_k$) direction. The designed beam pattern is achieved by using threshold values set to 1, 2 and 3 used in algorithm 1. The designed beam pattern is close to the desired beam pattern. Using the same procedure of waveform design for elevation angle which is used for azimuth angle. Figure 10 shows the Minimum Square Error (MSE) between desired beam pattern at $-40°$ to $-20°$ and from 20° to 40° in ($\phi_k$) direction.

### B. SPECTRUM SHARING BETWEEN RADAR AND COMMUNICATION SYSTEM THROUGH RELAY SYSTEMS

Considering the system model shown in Figure 1 and Figure 2. In the first case, the simulation results of SNR versus BER for two-hop DAF and three-hop (DF & AF) are compared. In the second case, the probability of detection for two-hop AF or DF or DAF with different relay positions between MIMO radar and MIMO communication systems are compared. In the third case, the probability of detection for three-hop (DF & AF) with different relay positions

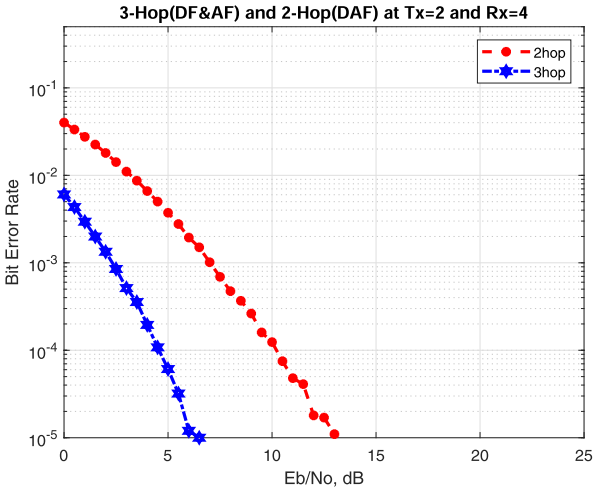


**FIGURE 12.** Performance evaluation of SNR versus BER for 2 and 3 hop relays system with Tx=2 & Rx = 4.

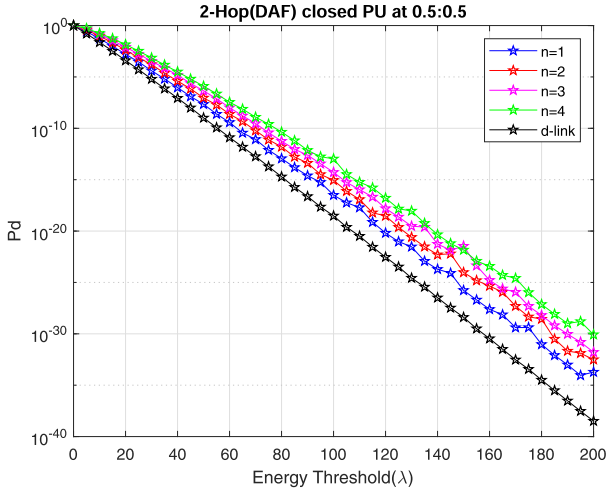


**FIGURE 13.** Performance evaluation of probability of detection versus energy threshold of 2 hop relay network PU at 05:05.

between MIMO radar and MIMO communication systems are also compared.

#### 1) CASE1: TWO-HOP DAF AND THREE-HOP (DF & AF)

Two-hop DAF relaying protocol and three-hop (DF & AF) relaying protocol are compared. The three-hop relaying protocol is implemented as DF in the first-hop and AF in the second-hop. The positioning of the relay in three-hop are in equal place from radars and communication system. Figure 11 and Figure 12 shows the simulation results for $2 \times 2$ and $2 \times 4$ two-hop DAF and three-hop (DF & AF) MIMO technique, respectively. The results are based on SNR in db versus BER. The results clearly show in both figures that the three-hop (DF & AF) have less BER as compared to two-hop DAF. The three-hop relaying protocol, in first-hop decodes and forwards the received signal from radar and sends the decoded signal to the other relay. The other relay of second-hop on receiving signal, just amplifies and sends to the communication system. Two-hop relaying

**TABLE 2.** Comparison of our proposed model with the state-of-the-art waveform design methods.

| S.NO | Authors | Covariance matrix matching problem | FACE property proved | Azimuth angle used | New additional elevation angle |
|---|---|---|---|---|---|
| **1** | Fuhrmann et al. | Suggested constant modulus waveforms through cross correlation matrix | Not proved | Yes | No |
| **2** | Aittomaki et al. | Suggested waveforms under total power constraint | Not proved | Yes | No |
| **3** | Gong et al. | Suggested omnidirectional beam pattern focussing on higher value for predetermined threshold values for main lobes | Not proved | Yes | No |
| **4** | Hua et al. | Suggested waveforms for energy focussing with a constraint on the energy of ripples | Not proved | Yes | No |
| **5** | Ahmed et al. | Suggested waveforms using BPSK & QPSK waveforms | proved but did not satisfy the constant Envelop Property | Yes | No |
| **6** | Sodagari et al. | Suggested mathematical proof for the covariance matrix of QPSK waveforms | Method Provided | Yes | No |
| **7** | Khawar et al. | Proved FACE property of QPSK waveforms | Proved and satisfied | Yes | No |
| **8** | Liu et al. | Constant modulus waveform design using singular value decomposition | Not proved | Yes | No |
| **9** | liu2018mu | Joint waveform design for all antennas shared by radar and communication | Not proved | Yes | Yes |
| **10** | **Our contribution** | **Target detection is improved through elevation angle and different relaying protocols used for spectrum sharing** | **Proved** | **Yes** | **Added** |

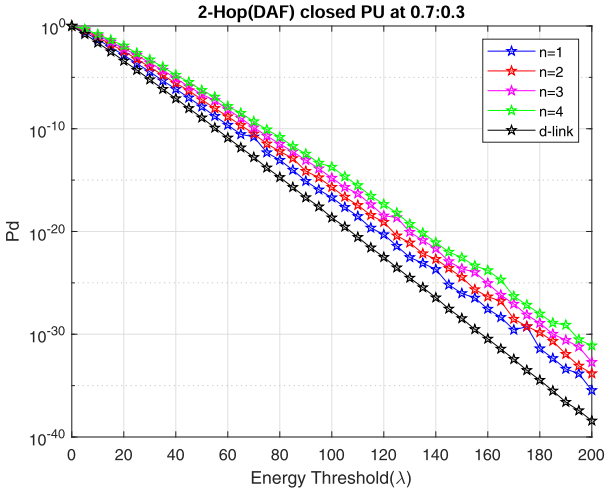


**FIGURE 14.** Performance evaluation of probability of detection versus energy threshold of 2 hop relay network PU at 07:03.

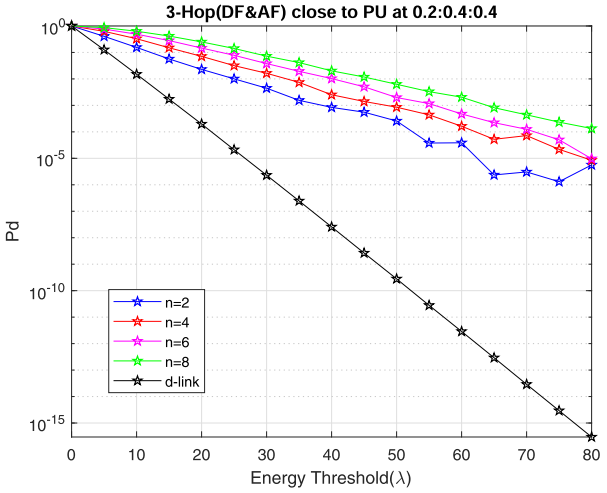


**FIGURE 15.** Performance evaluation of probability of detection versus energy threshold of 3 hop relay network PU at 02:04:04.

protocol has higher path-loss compared to three-hop, due to the positioning of the relay between radar and communication systems.

### 2) CASE2: PROBABILITY OF DETECTION FOR TWO-HOP AF, DF, DAF WITH DIFFERENT RELAY POSITIONS

Figure 13 and Figure 14 shows the simulation results of two-hop network for probability of detection for sensing of the radars signal with two different relays positions. In Figure 13, the relays are at equal positions i.e., 0.5:0.5, whereas in Figure 14, the relays are at a distance of 0.7:0.3 from MIMO radar and MIMO communication systems.

### 3) CASE3: PROBABILITY OF DETECTION FOR THREE-HOP (DF & AF) WITH DIFFERENT RELAY POSITIONS

Figure 15 and Figure 16 shows the simulation results of three-hop network for probability of detection for sensing of the radars signal with two different relays positions. In Figure 15, the relays are at a distance of 0.2:0.4:0.4, whereas in Figure 16, the relays are at a distance of 0.4:0.4:0.2 from MIMO radar and communication systems.

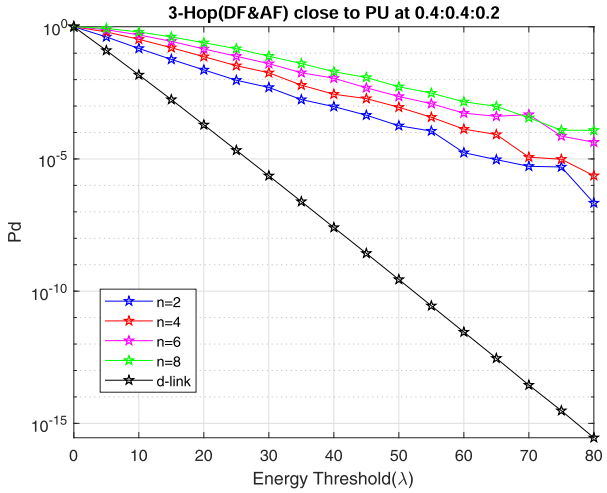


**FIGURE 16.** Performance evaluation of probability of detection versus energy threshold of 3 hop relay network PU at 04:04:02.

We formulate the probability of detection for the radars signal as,

$$P_d \propto Number\ of\ hopes,\ Number\ of\ relays \tag{52}$$

$$P_d \propto \frac{1}{distance\ of\ relay\ from\ PU} \tag{53}$$

Table 2 shows the comparison for the waveform design approach carried out by different researchers. The waveform design is carried on a covariance matrix matching problem, which is based on FACE property. All of the researchers either have not proven the FACE property or have proved through the azimuth angle only. Our contribution in waveform design approach is the addition of an elevation angle, which in addition can detect the target in the air while previously the target could be detected in ground plane only.

## IV. CONCLUSION

The work presented in this paper has resolved the problem of detecting the target involving two angles which includes the azimuth and elevation angles, while keeping the constraint of FACE beam pattern design. Radar can detect a target in air through azimuth and elevation angles with some probability "$p$" as it was zero in previous work in the literature. Besides waveform design, the radar is also capable of sharing its available spectrum with the communication system. SNR versus BER is computed for the efficient performance of the system. The results show that three-hop (DF & AF) has lower BER compared to two-hop relaying protocols. Furthermore, the probability of detection of three-hop (DF & AF) is higher compared to two-hop systems by keeping a minimum distance of relays from the PU.

## REFERENCES

[1] *National Broadband Plan*, Federal Commun. Commission, Washington, DC, USA, 2010.
[2] M. Cotton, J. Wepman, J. Kub, S. Engelking, Y. Lo, H. Ottke, R. Kaiser, D. Anderson, M. Souryal, and M. Ranganathan, "An overview of the NTIA/NIST spectrum monitoring pilot program," in *Proc. IEEE Wireless Commun. Netw. Conf. Workshops (WCNCW)*, Mar. 2015, pp. 217–222.
[3] M. R. Bell, N. Devroye, D. Erricolo, T. Koduri, S. Rao, and D. Tuninetti, "Results on spectrum sharing between a radar and a communications system," in *Proc. Int. Conf. Electromagn. Adv. Appl. (ICEAA)*, Aug. 2014, pp. 826–829.
[4] D. Erricolo, H. Griffiths, L. Teng, M. C. Wicks, and L. Lo Monte, "On the spectrum sharing between radar and communication systems," in *Proc. Int. Conf. Electromagn. Adv. Appl. (ICEAA)*, Aug. 2014, pp. 890–893.
[5] M. M. Kassem and M. K. Marina, "Future wireless spectrum below 6 GHz: A UK perspective," in *Proc. IEEE Int. Symp. Dyn. Spectr. Access Netw. (DySPAN)*, Sep. 2015, pp. 59–70.
[6] T. Wang, G. Li, B. Huang, Q. Miao, J. Fang, P. Li, H. Tan, W. Li, J. Ding, J. Li, and Y. Wang, "Spectrum analysis and regulations for 5G," in *5G Mobile Communications*. Cham, Switzerland: Springer, 2017, pp. 27–50.
[7] A. Lackpour, M. Luddy, and J. Winters, "Overview of interference mitigation techniques between WiMAX networks and ground based radar," in *Proc. 20th Annu. Wireless Opt. Commun. Conf. (WOCC)*, Apr. 2011, pp. 1–5.
[8] *Enabling Innovative Small Cell Use in 3.5 Ghz Band NPRM & Order*, document FCC 12 148, Federal Commun. Commission, 2012.
[9] Q. Zhao and B. M. Sadler, "Dynamic spectrum access: Signal processing, networking, and regulatory policy," 2006, *arXiv:cs/0609149*. [Online]. Available: https://arxiv.org/abs/cs/0609149
[10] R. Saruthirathanaworakun, J. M. Peha, and L. M. Correia, "Performance of data services in cellular networks sharing spectrum with a single rotating radar," in *Proc. IEEE Int. Symp. a World Wireless, Mobile Multimedia Netw. (WoWMoM)*, Jun. 2012, pp. 1–6.
[11] F. Liu, A. Garcia-Rodriguez, C. Masouros, and G. Geraci, "Interfering channel estimation in radar-cellular coexistence: How much information do we need?" *IEEE Trans. Wireless Commun.*, vol. 18, no. 9, pp. 4238–4253, Jun. 2019.
[12] H. Deng and B. Himed, "Interference mitigation processing for spectrum-sharing between radar and wireless communications systems," *IEEE Trans. Aerosp. Electron. Syst.*, vol. 49, no. 3, pp. 1911–1919, Jul. 2013.
[13] S. Sodagari, A. Khawar, T. Charles Clancy, and R. McGwier, "A projection based approach for radar and telecommunication systems coexistence," in *Proc. IEEE Global Commun. Conf. (GLOBECOM)*, Dec. 2012, pp. 5010–5014.
[14] A. Khawar, A. Abdel-Hadi, and T. Charles Clancy, "MIMO radar waveform design for coexistence with cellular systems," in *Proc. IEEE Int. Symp. Dyn. Spectr. Access Netw. (DYSPAN)*, Apr. 2014, pp. 20–26.
[15] F. Liu, C. Masouros, and H. Griffiths, "Dual-functional radar-communication waveform design under constant-modulus and orthogonality constraints," in *Proc. Sensor Signal Process. Defence Conf. (SSPD)*, May 2019, pp. 1–5.
[16] J. Tan and G. L. Stuber, "Constant envelope multi-carrier modulation," in *Proc. MILCOM*, vol. 1. 2002, pp. 607–611.
[17] P. Stoica, J. Li, and X. Zhu, "Waveform synthesis for diversity-based transmit beampattern design," *IEEE Trans. Signal Process.*, vol. 56, no. 6, pp. 2593–2598, Jun. 2008.
[18] S. C. Thompson, A. U. Ahmed, J. G. Proakis, J. R. Zeidler, and M. J. Geile, "Constant envelope OFDM," *IEEE Trans. Commun.*, vol. 56, no. 8, pp. 1300–1312, Aug. 2008.
[19] S. Ahmed, J. S. Thompson, Y. R. Petillot, and B. Mulgrew, "Finite alphabet constant-envelope waveform design for MIMO radar," *IEEE Trans. Signal Process.*, vol. 59, no. 11, pp. 5326–5337, Nov. 2011.
[20] S. Sodagari and A. Abdel-Hadi, "Constant envelope radar with coexisting capability with LTE communication systems," *IEEE Trans. Wireless Commun.*, to be published.
[21] A. Khawar, A. Abdelhadi, and T. Charles Clancy, "Target detection performance of spectrum sharing MIMO radars," 2014, *arXiv:1408.0540*. [Online]. Available: http://arxiv.org/abs/1408.0540
[22] A. Khawar, A. Abdel-Hadi, and T. Charles Clancy, "Spectrum sharing between S-band radar and LTE cellular system: A spatial approach," in *Proc. IEEE Int. Symp. Dyn. Spectr. Access Netw. (DYSPAN)*, Apr. 2014, pp. 7–14.
[23] A. Khawar, A. Abdelhadi, and T. C. Clancy, "QPSK waveform for MIMO radar with spectrum sharing constraints," *Phys. Commun.*, vol. 17, pp. 37–57, Dec. 2015.
[24] A. Babaei, W. H. Tranter, and T. Bose, "A nullspace-based precoder with subspace expansion for radar/communications coexistence," in *Proc. IEEE Global Commun. Conf. (GLOBECOM)*, Dec. 2013, pp. 3487–3492.
[25] S. Atapattu, C. Tellambura, and H. Jiang, "Relay based cooperative spectrum sensing in cognitive radio networks," in *Proc. IEEE Global Telecommun. Conf. (GLOBECOM)*, Dec. 2009, pp. 1–5.

[26] M. Kamal, M. Ibrahim, S. Mir, and M. Naveed Aman, "Comparison of multihop relaying protocols in cognitive radio networks," in *Proc. 6th Int. Conf. Innov. Comput. Technol. (INTECH)*, Aug. 2016, pp. 611–616.
[27] J. Li and P. Stoica, "MIMO radar with colocated antennas," *IEEE Signal Process. Mag.*, vol. 24, no. 5, pp. 106–114, Sep. 2007.
[28] B. Li, A. P. Petropulu, and W. Trappe, "Optimum co-design for spectrum sharing between matrix completion based MIMO radars and a MIMO communication system," *IEEE Trans. Signal Process.*, vol. 64, no. 17, pp. 4562–4575, 2016.
[29] B. Li and A. P. Petropulu, "Joint transmit designs for coexistence of MIMO wireless communications and sparse sensing radars in clutter," *IEEE Trans. Aerosp. Electron. Syst.*, vol. 53, no. 6, pp. 2846–2864, Dec. 2017.
[30] F. Liu, C. Masouros, A. Li, and T. Ratnarajah, "Robust MIMO beamforming for cellular and radar coexistence," *IEEE Wireless Commun. Lett.*, vol. 6, no. 3, pp. 374–377, Jun. 2017.
[31] F. Liu, C. Masouros, A. Li, T. Ratnarajah, and J. Zhou, "MIMO radar and cellular coexistence: A power-efficient approach enabled by interference exploitation," *IEEE Trans. Signal Process.*, vol. 66, no. 14, pp. 3681–3695, 2018.
[32] F. Liu, C. Masouros, A. Li, H. Sun, and L. Hanzo, "MU-MIMO communications with MIMO radar: From co-existence to joint transmission," *IEEE Trans. Wireless Commun.*, vol. 17, no. 4, pp. 2755–2770, Apr. 2018.
[33] J. Liu, K. Vijay Mishra, and M. Saquib, "Co-designing statistical MIMO radar and in-band full-duplex multi-user MIMO communications," 2020, *arXiv:2006.14774*. [Online]. Available: http://arxiv.org/abs/2006.14774
[34] F. Liu, L. Zhou, C. Masouros, A. Li, W. Luo, and A. Petropulu, "Toward dual-functional radar-communication systems: Optimal waveform design," *IEEE Trans. Signal Process.*, vol. 66, no. 16, pp. 4264–4279, 2018.
[35] D. R. Fuhrmann and G. San Antonio, "Transmit beamforming for MIMO radar systems using signal cross-correlation," *IEEE Trans. Aerosp. Electron. Syst.*, vol. 44, no. 1, pp. 171–186, Jan. 2008.
[36] T. Aittomaki and V. Koivunen, "Signal covariance matrix optimization for transmit beamforming in MIMO radars," in *Proc. Conf. Rec. 41st Asilomar Conf. Signals, Syst. Comput.*, Nov. 2007, pp. 182–186.
[37] P. Gong, Z. Shao, G. Tu, and Q. Chen, "Transmit beampattern design based on convex optimization for mimo radar systems," *Signal Process.*, vol. 94, pp. 195–201, Jan. 2014.
[38] G. Hua and S. S. Abeysekera, "MIMO radar transmit beampattern design with ripple and transition band control," *IEEE Trans. Signal Process.*, vol. 61, no. 11, pp. 2963–2974, 2013.
[39] B. Misra and A. Deb, "Synthesis of antenna arrays with flat-top pattern using conventional and random drift particle swarm optimization algorithms," in *Proc. Emerg. Trends Electron. Devices Comput. Techn. (EDCT)*, Mar. 2018, pp. 1–5.
[40] F. Liu, C. Masouros, A. P. Petropulu, H. Griffiths, and L. Hanzo, "Joint radar and communication design: Applications, state-of-the-art, and the road ahead," *IEEE Trans. Commun.*, vol. 68, no. 6, pp. 3834–3862, Jun. 2020.

**SULEMAN MIR** received the B.S. degree in telecommunication engineering from the National University of Computer and Emerging Sciences, Peshawar, Pakistan, in 2007, and the M.S. degree in electrical engineering from the University of Leeds, Leeds, England, in 2012. He is currently pursuing the Ph.D. degree in electrical engineering with the National University of Computer and Emerging Sciences. After graduation, he got expertise in microwave backhaul communication system. His expertise includes link planning, installing and commissioning links, and system trouble shooting. Since 2012, he has been working as an Assistant Professor with the National University of Computer and Emerging Sciences. His research interests include waveform design, spectrum sharing, cooperative communication, and cognitive radio networks.

**INAM BARI** (Senior Member, IEEE) received the B.S. degree (Hons.) in telecommunication engineering from the National University of Computer and Emerging Sciences (NUCES), Peshawar, in 2007, and the Ph.D. degree in electronics and communication engineering from the Politecnico di Torino, Italy, in 2014, through a fully funded five years scholarship for M.S. leading to Ph.D. awarded from the Higher Education Commission (HEC), Pakistan. He started his professional career as a Laboratory Engineer with NUCES after completion his B.S. degree. He worked as an Assistant Professor and the Head of the Department with NUCES. In 2014, he joined NUCES Peshawar Campus again as an Assistant Professor with the Department of Electrical Engineering. He is currently a Lecturer with the Systems Engineering Department, Military Technological College, Muscat, Oman. He is in collaboration with many prestigious organization, including California State University Los Angles (CSULA), USA, the Istituto Nazionale di Ricerca Metrologica (INRIM), and Ben Gurion University of the Negev, Beer-Sheva, Israel. He has coauthored numerous conference articles, journal articles, and a book chapter in the aforementioned topics. He has received several grants and awards from various funding agencies, including NATO and Telecom Italia. He is a HEC approved Ph.D. supervisor with research interests include information reconciliation, channel modelling, channel coding, soft decoding for Quantum Key Distribution (QKD), optical communication, and optical switching and spectrum sharing in next generation cellular communication. His current research project which focus on interdisciplinary applications of Physics and Engineering is a collaboration between NATO countries and partner countries where he is working as a co-director and represent Pakistan and NUCES. He is a member of IET.

**MOHSIN KAMAL** (Senior Member, IEEE) received the B.S. degree in telecommunication engineering from the National University of Computer and Emerging Sciences, Peshawar, Pakistan, in 2008, the M.S. degree in electrical engineering from Blekinge Tekniska Högskola, Karlskrona, Sweden, in 2012, and the Ph.D. degree in electrical engineering from the National University of Computer and Emerging Sciences.

Since 2013, he has been working as an Assistant Professor with the National University of Computer and Emerging Sciences. His research interests include development of light-weight solutions for various IoT applications, wireless sensor networks, cooperative communication, and cognitive radio networks. He has been the IEEE Student Branch Counselor with the National University of Computer and Emerging Sciences, since 2016. Besides that, he is elected as a Secretary of IEEE Peshawar subsection from January 2019.

**HAIDER ALI** (Senior Member, IEEE) was born in 1984. He received the B.S. degree in telecommunication engineering from NUCES, Pakistan, in 2007, and the M.S. degree in electronics engineering and the Ph.D. degree in electronics and communication engineering from the Politecnico di Torino, Italy, in 2010 and 2014, respectively. He is currently working as an Assistant Professor with the Department of Department of Electrical and Electronics Engineering, University of Technology, Nowshera, Pakistan. His research interests include data acquisition systems for thermal measurements, power electronics, renewable energy systems and materials, design and development of antenna, radio frequency (RF) front end, and telecommunication subsystem for small satellites.